Cu^+ in Liquid Ammonia and in Water: Intermolecular Potential Function and Monte Carlo Simulation

Harno D. Pranowo,[†] A. H. Bambang Setiaji,[†] and Bernd M. Rode*

Theoretical Chemistry Division, Institute of General, Inorganic and Theoretical Chemistry, University of Innsbruck, A-6020 Innsbruck, Austria

Received: July 15, 1999; In Final Form: October 8, 1999

The solvation structure of Cu^+ in water and in liquid ammonia has been investigated using the Metropolis Monte Carlo method. The systems consisting of one Cu^+ in 215 solvent molecules have been simulated at a temperature of 240 K for ammonia and 298 K for water, respectively. Cu^+−ammonia and Cu^+−water pair potentials have been newly developed based on ab initio calculations of double-ζ quality. Structural properties were investigated by means of radial distribution functions and their running integration numbers, leading for the first solvation shell to an average coordination number 6 and Cu−N distance of 2.20 Å in ammonia, and to number 6 and Cu−O distance of 2.20 Å in water. The RDFs, coordination number distributions, and pair interaction energy distribution analyses indicate that ligand exchange reactions take place more easily in water than in liquid ammonia.

1. Introduction

Binding of Cu^+ to small molecules has been the focus of several experimental and theoretical studies. These include complexes of Cu^+ with one and more molecules of water[1−7] and/or ammonia.[8−10]

Holland and Castleman[11] reported on the basis of high-pressure mass spectroscopy that copper forms a $[Cu(H_2O)_4]^+$ cluster in the gas phase, but no experimental data is available for Cu^+ in aqueous solution, probably due to the low solubility of its salts in water. Stevenson and his group[12,13] studied the triaminocopper(I) complex in aqueous ammonia using ultraviolet spectroscopy. The stability constants for the stepwise formation of $[Cu(NH_3)_3]^+$ were determined at 1 M ionic strength, resulting in an overall value of 0.05. The preferred Cu^+ species in aqueous ammonia solution is $[Cu(NH_3)_2]^+$ with a stability constant of 0.86×10^5 at 2 M ionic strength. So far, there is no experimental data referring to the microscopic structure of these complexes.

The structural and energetic features of the hydration of Cu^+ in aqueous solution have been studied by Monte Carlo simulation, resulting in a coordination number of six for the first hydration shell of the Cu^+,[14] corresponding to an octahedral structure in the first shell. The structure of a second hydration shell of Cu^+ could not be described because of the use of only 20 water molecules in this simulation.

In most simulations, pair interaction potentials have been used to describe ion−ligand interactions. It is known, however, that the assumption of pairwise additivity can lead to serious errors in the description of ions in water[4,15,16] and liquid ammonia[17−19] as well, especially for doubly charged cations, as a significant part of the many-body effects is due to polarization effects.[20] The Cu^{2+}−NH_3 and Cu^{2+}−H_2O ab initio pair potentials are inadequate to describe the solvation structure of Cu^{2+}, leading especially to an overestimation of the coordination number (8 instead of 6) and of hydration energies.[15,18] The inclusion of three-body interactions markedly improves the agreement with experimental data.[21]

The electrostatic interaction between Cu^+ and ligands should be much weaker than in the case of the doubly charged cation Cu^{2+}, so that the neglect of 3-body effects seemed acceptable for the present work, especially after some ab initio calculations of $[Cu(NH_3)_n]^+$ and $[Cu(H_2O)_n]^+$ complexes had been performed in order to estimate their order of magnitude. Pair potential based Monte Carlo simulations were performed, therefore, for systems consisting of one Cu^+ and 215 ammonia molecules and one Cu^+ and 215 water molecules, respectively. The results are reported and discussed in terms of structural properties and compared with other theoretical and experimental investigations.

2. Details of the Calculations

2.1. Estimation of Many-Body Effects. To investigate the influence of many-body terms on the interactions between Cu^+ and water and ammonia, ab initio calculations with energy optimization of $Cu(L)_n^+$ complexes, where L is H_2O or NH_3, and $n = 1-6$, were carried out using the double-ζ valence (DZV) basis set of Schäfer et al.[22] for copper. The double-ζ plus polarization (DZP) basis sets of Dunning[23] corresponding to D95V* in the *Gaussian 94* program[24] were used for water and ammonia. The experimental gas-phase geometries of the ammonia molecule[25] with N−H distance of 1.0124 Å and HNH angle of 106.67° and for water[26] with O−H distance of 0.9601 Å and H−O−H angle of 104.47° were taken as starting values for the optimization.

The stabilization energies of the complexes, ΔE_{stb}, were calculated as

$$\Delta E_{stb} = E_{ML_n} - E_M - E_{L_n} \quad (1)$$

where E_{ML_n}, E_M, and E_{L_n} are the total energies of $[Cu(NH_3)_n]^+$ or $[Cu(H_2O)_n]^+$, Cu^+ and n NH_3 or H_2O molecules in the same configuration as that of the $[Cu(L)_n]^+$ complexes, respectively.

[†] Permanent address: Austrian-Indonesian Centre for Computer Chemistry, Gadjah Mada University, Yogyakarta, Indonesia.

10.1021/jp992410j CCC: $18.00
Published on Web 11/23/1999

TABLE 1: Final Optimized Parameters for the Interactions of N and H Atoms of Ammonia and of O and H Atoms of Water with Cu^{+a}

pair	charge	*A*	*B*	*C*	*D*
Cu^+-NH_3	(a.u.)	(kcal mol^{-1} Å^6)	(kcal mol^{-1} Å^8)	(kcal mol^{-1})	(Å^{-1})
Cu−N	−0.8022	−7898.9937	6436.6190	119469.5589	3.6357
Cu−H	0.2674	−1401.6483	1402.2589	5468.8967	2.7279
Cu^+-H_2O	(a.u.)	(kcal mol^{-1} Å^5)	(kcal mol^{-1} Å^8)	(kcal mol^{-1})	(Å^{-1})
Cu−O	−0.6598	−1113.5410	948.7345	61435.4148	3.8498
Cu−H	0.3299	−328.7231	223.0600	4196.7013	2.9325

[a] The atomic net charges are given in a.u., interaction energies and distances in kcal mol^{-1} and Å, respectively.

TABLE 2: Optimized Geometries and Corresponding Many-Body Effects in $Cu(NH_3)_n^+$ and $Cu(H_2O)_n^+$ Complexes

Cu^+-NH_3

n	r_{Cu-N}	r_{N-H}	$\angle_{HNH}$	ΔE_{stb}	ΔE_{avbin}	ΔE_{avpi}	$\%\Delta E_{avpi}$	ΔE_{rpl}
1	2.08	1.01	106.0	−43.4	−43.3	−43.4	0.0	0.0
2	2.05	1.01	106.0	−87.8	−43.8	−43.6	0.6	3.1
3	2.18	1.01	106.0	−113.7	−37.8	−41.7	9.2	10.0
4	2.28	1.01	106.1	−136.7	−34.1	−39.8	14.2	19.6
6	2.53	1.01	106.4	−163.0	−27.1	−37.3	27.2	41.8

Cu^+-H_2O

n	r_{Cu-O}	r_{O-H}	$\angle_{HOH}$	ΔE_{stb}	ΔE_{avbin}	ΔE_{avpi}	$\%\Delta E_{avpi}$	ΔE_{rpl}
1	2.07	0.95	107.0	−33.4	−33.4	−33.4	0.0	0.0
2	2.05	0.95	107.3	−66.3	−33.1	−33.2	0.3	1.4
3	2.15	0.95	106.8	−89.3	−29.8	−32.1	7.0	5.7
4	2.24	0.95	106.8	−109.7	−27.4	−30.9	11.3	11.6
6	2.42	0.95	106.6	−140.3	−23.4	−29.4	20.5	30.0

The average binding energy per ligand molecule, ΔE_{avbind}, is computed as

$$\Delta E_{avbind} = \Delta E_{stb}/n \quad (2)$$

To evaluate possible errors of the assumption of pairwise additivity of interactions due to many-body effects, average pair interaction energies between M and L in ML_n complexes, ΔE_{avpi} were calculated and defined as

$$\Delta E_{avpi} = \sum_{i=1}^{n} [E_{ML_i} - E_M - E_{L_i}]/n \quad (3)$$

where ML_i denotes any of the ML pairs in the ML_n complexes. The percentage of nonadditivity, $\%E_{avpi}$, was then defined as

$$\%E_{avpi} = 100(1 - \Delta E_{avbin}/\Delta E_{avpi}) \quad (4)$$

The repulsion energy between ligands is calculated as

$$\Delta E_{rpl} = E_{L_n} - nE_L \quad (5)$$

The results of geometry optimization and the data for estimating many-body effects are given in Table 2.

2.2. Construction of the Pair Potentials. To construct the Cu^+-NH_3 and Cu^+-H_2O pair potentials, the ligand molecule was fixed in the origin of the coordinate system and Cu^+ was moved in configuration sphere varying geometrical parameters within 1.5 Å $\le r_{Cu-L} \le$ 15.0 Å, $0° \le \theta \le 180°$ and $0° \le \phi \le 60°$ (Figure 1). The interaction energies, ΔE_{2b}, between Cu^+−ammonia and Cu^+−water were computed by subtracting the ab initio energies of the isolated species E_{Cu} and E_L from those of the monosolvates E_{CuL}, where L denotes ammonia or water

$$\Delta E_{2b} = E_{CuL^+} - E_{Cu^+} - E_L \quad (6)$$

Both pair potentials were developed from more than 900 SCF energy points for Cu^+−ammonia and Cu^+−water, respectively. The fitting process to an analytical potential function was performed by the least-squares method with Levenberg−Marquart algorithm, with various potential types. The best analytical potential function form describing all electronic and van der Waals interactions resulted as

$$\Delta E_{FIT} = \sum_{i=1}^{4} A_{iM} r_{iM}^{-6} + B_{iM} r_{iM}^{-8} + C_{iM} \exp(-D_{iM} r_{iM}) + q_i q_M r_{iM}^{-1} \quad (7)$$

for Cu^+-NH_3 pair potential and

$$\Delta E_{FIT} = \sum_{i=1}^{3} A_{iM} r_{iM}^{-5} + B_{iM} r_{iM}^{-8} + C_{iM} \exp(-D_{iM} r_{iM}) + q_i q_M r_{iM}^{-1} \quad (8)$$

for Cu^+-H_2O pair potential, where A_{iM}, B_{iM}, C_{iM}, and D_{iM} denote the fitting parameters, r_{iM} are distances between the *i*th atom of the ligand and Cu^+, q_i are the net charges of the *i*th atom of the ligand obtained by Mulliken population analysis, and q_M is the atomic net charge of Cu^+. Weight factors were introduced to give special emphasis to values near the global and local energy minima and repulsive, destabilized configurations with energies above 50 kcal mol^{-1} were excluded. The standard deviations of the fitted values from SCF data were ±1.3 kcal mol^{-1} and ±2.1 kcal mol^{-1} for the Cu^+−water system and Cu^+−ammonia system, respectively. This analytical potential function form is in analogy to the form of potential functions previously constructed for other solvated metal ions.[17,27−29]

In the pair potential construction, artificial charge-transfer effects at larger ion−ligand distance have been observed for Cu^+−water[35,36] and Cu^+−ammonia.[18] The ECP-DZP basis sets proposed by Stevens et al.[37] or Hay and Wadt[38] for Cu^+ also produced very large charge-transfer effects and thus gave partially erroneous energies at larger ion−ligand distances. For example, calculations using the basis set proposed by Stevens et al.[37] show that the total Cu^+−ammonia complex energy, where $\theta = 0°$ and $\phi = 0°$ (Figure 1), changes from −206.4 au to −140.0 au upon increasing the Cu−N distance from 6 to 7 Å, one to be the formation of Cu and NH_3^+. Such charge-transfer effects were not observed when the VDZ basis set proposed by Schäfer et al.[22] was used for copper. The global minimum of −43.4 kcal mol^{-1} of the Cu^+-NH_3 system was considerably higher than the experimental result (−49.34 kcal mol^{-1}),[39] whereas for Cu^+-H_2O the global minimum resulted only 1.4 kcal mol^{-1} above the experimental value[2] of −35.0 kcal mol^{-1}. The larger discrepancy in the case of NH_3 might be due to the larger charge-transfer effects as well as to a larger error in comparison to water, using a noncorrelated wave function.

2.3. Monte Carlo Simulations. One Monte Carlo simulation was performed for a system consisting of one Cu^+ and 215 NH_3

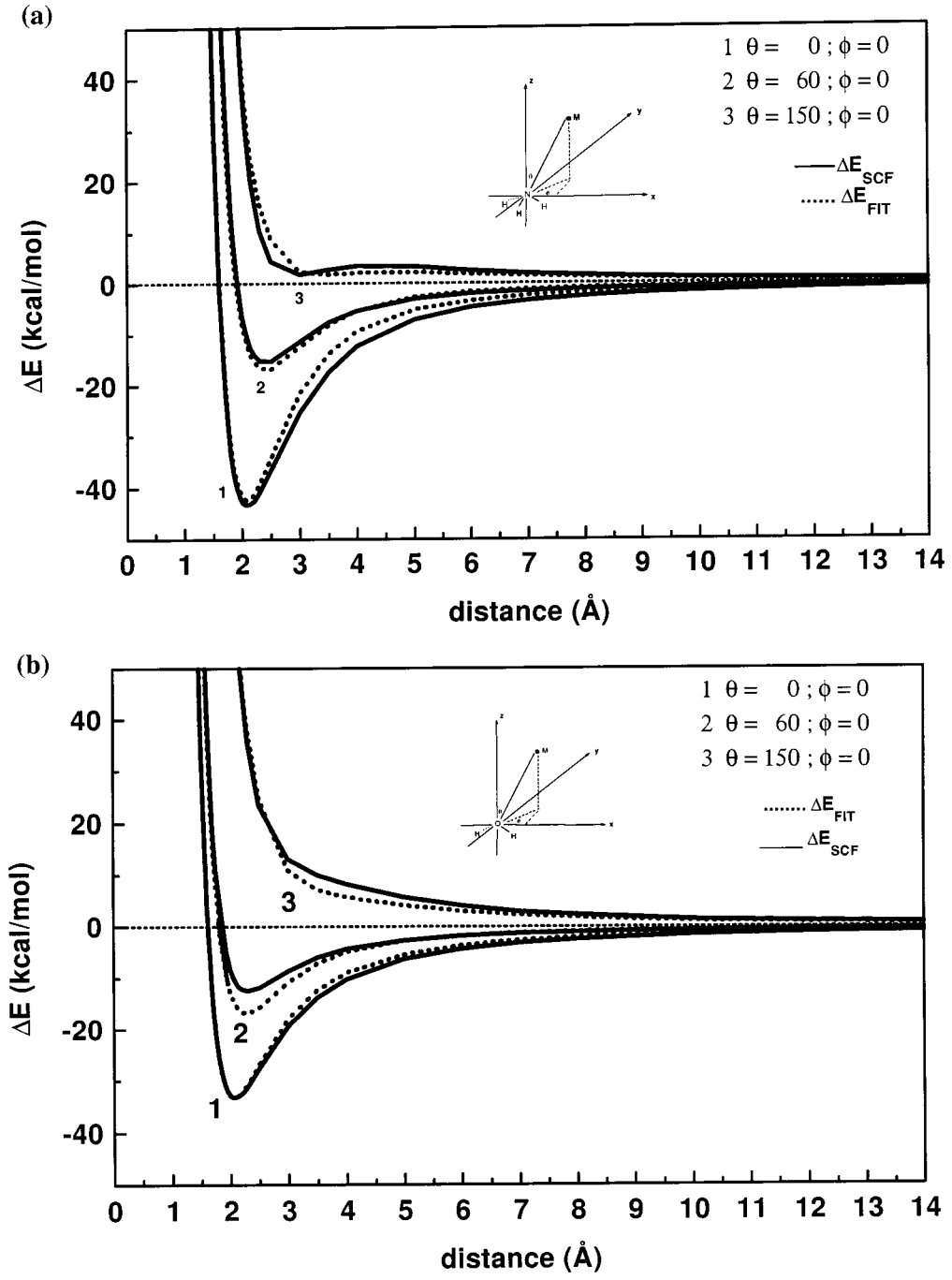

Figure 1. Comparison of the energies obtained from the SCF calculations, ΔE_{SCF}, and from the potential function, ΔE_{FIT}, for (a) Cu^+−ammonia system and (b) Cu^+−water system, using the final values of the fitting parameters as given in Table 2 for values of $\theta = 0°$, 60° and 150°, and $\phi = 0°$.

using the newly developed two-body function at temperature of 240 K. Ammonia−ammonia interactions were described by a function taken from literature.[29] A periodic box length of 20.8546 Å was set in accordance with the experimental density of pure liquid ammonia at 240 K and 1 atm (0.682 g cm^{-3}). A second simulation was performed for Cu^+ in water, with one Cu^+ and 215 water molecules placed in the elementary box. At the temperature of 298 K, the edge length of this box is 18.7170 Å, corresponding to the density of pure water (0.997 g cm^{-3}). For water−water interactions, the CF2 potential proposed by Jancso and Heinzinger[30] was used. Periodic boundary condition and cutoff of exponential terms at half of this length were applied.[31] After generating a starting configuration randomly, the systems had reached energetic equilibrium after 3 million configurations, setting an acceptance ratio of 1:3. For the evaluation of structural data a further 3 million configurations were sampled.

3. Results and Discussion

3.1. Role of Non-Additive Terms. Table 2 shows that the Cu−N and Cu−O distances increase and the stabilization energy per ligand molecule, ΔE_{avbin}, decreases as expected with larger *n*. The elongation of Cu−L can be understood from the ligand−ligand repulsion (ΔE_{rpl}). An exception is the $[Cu(NH_3)_2]^+$ complex, where this repulsion seems to be overcome by neutral polarization effects, leading to a slightly higher binding energy per ammonia molecule than in the case of a single ligand. Therefore, ΔE_{avbin} is more negative for $[Cu(NH_3)_2]^+$ than for $[Cu(NH_3)]^+$ and the Cu−N distance in $[Cu(NH_3)_2]^+$ is slightly

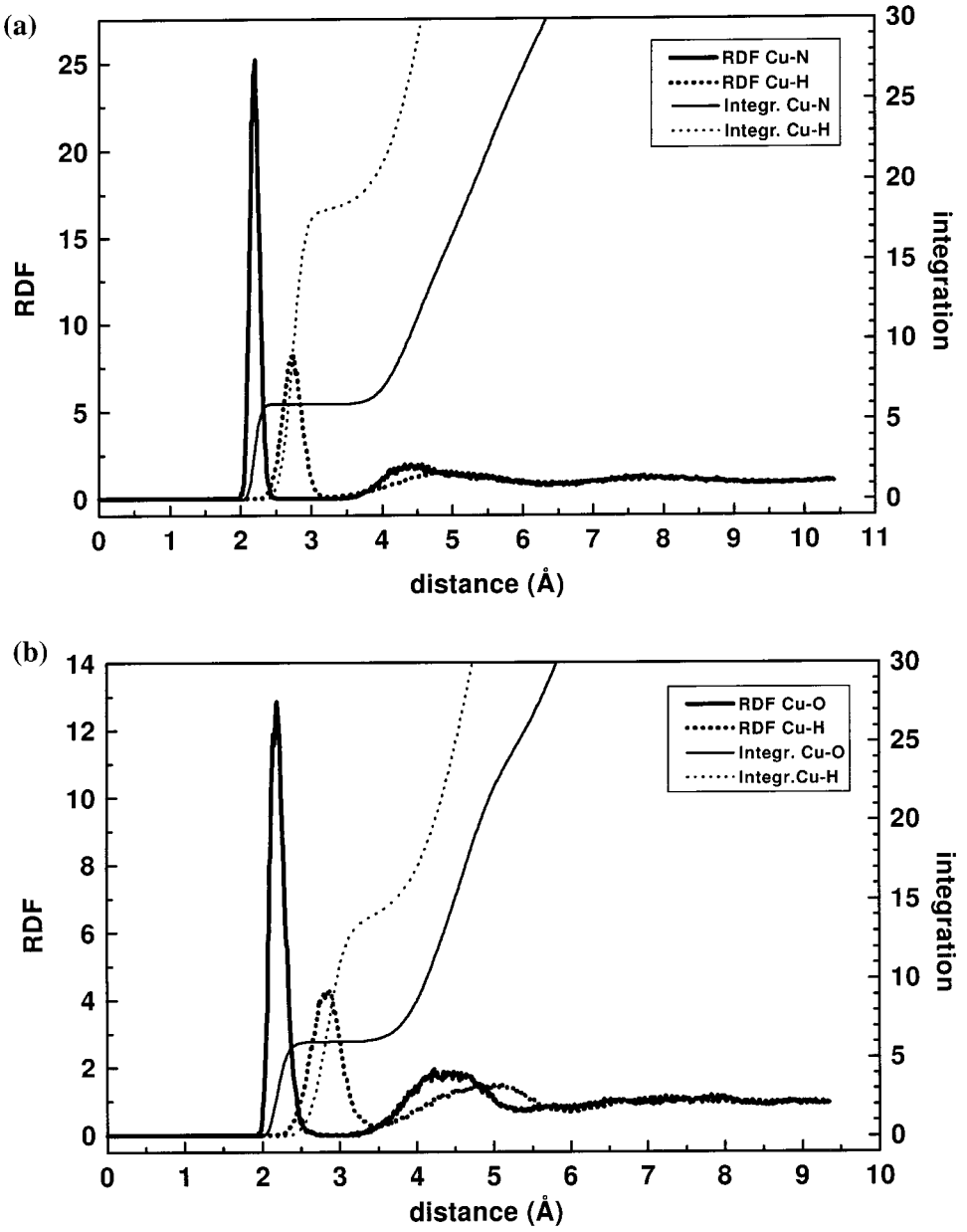

Figure 2. (a) Cu−N, Cu−H, and (b) Cu−O, Cu−H radial distribution functions and their running integration numbers for Cu^+−ammonia system at 240 K and Cu^+−water system at 298 K, respectively.

smaller than in $[Cu(NH_3)]^+$. This unusual feature has recently been reported in some experimental[2,3] and theoretical[5,8] studies on solvation of transition metal cations including Cu^+ and should be attributed to a cooperative effect, similar to that found in hydrogen bonding.[16]

Table 2 also shows that the assumption of pairwise additivity of Cu^+ complexes interaction energy may lead to a maximum error ($\%\Delta E_{avpi}$) of 27.2% and 20.5% for $[Cu(NH_3)_6]^+$ and $[Cu(H_2O)_6]^+$ complexes, respectively. The ammonia value is higher than in the case of other singly charged cation ammonia complexes namely $[K(NH_3)_6]^+$ (19%[28]), $[Li(NH_3)_6]^+$ (23%[33]), and $[Na(NH_3)_6]^+$ (17%[33]). The values for the hydrated complexes $[K(H_2O)_6]^+$ (17% [34]), $[Li(H_2O)_6]^+$ (20%[32]), and $[Na(H_2O)_6]^+$ (20%[34]) are rather similar, however. In complexes with doubly charged cation, the corresponding values are considerably higher, e.g., 30% for $[Mg(NH_3)_6]^{2+}$ [33] or 32% for $[Ca(H_2O)_6]^{2+}$.[34] Comparing these values, it still seemed acceptable to perform simulations with pair potentials alone, as they could be expected to lead to at least qualitatively correct results. For investigation on more details, however, a mixed QM/MM simulation[27,32] appears favorable. Such a simulation will consume, however, approximately 100 times more computer time.

3.2. Structural Data. The radial distribution functions (RDFs) for Cu−N/Cu−H in ammonia and Cu−O/ Cu−H in water, together with their corresponding running integration numbers are shown in Figure 2(a) and (b), respectively, and the characteristic values are summarized in Table 3.

The ammonia−ammonia and water−water RDFs are almost identical to those of liquid ammonia and pure water, respectively, and therefore only listed by their characteristic values in Table 3.

The first solvation sphere of Cu^+ in liquid ammonia is represented by a sharp peak of the Cu−N RDF, centered at 2.20 Å, 0.1 Å beyond the minimum of the SCF Cu^+−NH_3 potential, and 0.33 Å shorter than the optimized Cu−N distance for the $[Cu(NH_3)_6]^+$ complex. The average coordination number for the first solvation shell integrated up to the first minimum of 2.53 Å is 6, and only 0.03% of Cu^+ has a different

TABLE 3: Characteristic Values of the Radial Distribution Functions, $g_{\alpha\beta}(r)$ for the Cu^+−ammonia and Cu^+−water[a]

$\alpha\beta$	r_{M1}	r_{m1}	$n_{\alpha\beta}$(m1)	r_{M2}	r_{m2}	$n_{\alpha\beta}$(m2)
Cu^+−**NH_3**						
Cu N	2.20	2.53	5.99	4.32	6.41	23.54
Cu H	2.74	3.32	18.29	4.97	6.66	97.63
N N	3.38	5.02	12.03	6.55	8.04	51.17
N H	3.61	5.17	39.04	6.68	8.20	162.60
H H	3.83	5.22	40.07	6.82	8.45	171.32
Cu^+−**H_2O**						
Cu O	2.20	2.75	5.99	4.22	5.41	19.25
Cu H	2.92	3.48	14.13	5.03	6.01	63.26
O O	2.86	3.31	4.32	4.49	5.76	25.31
O H	1.94	2.48	1.89	3.20	6.03	58.63
H H	2.28	3.01	5.52	3.73	5.42	42.41

[a] r_{M1}, r_{M2} and r_{m1}, r_{m2} are the distances, in Å, where $g_{\alpha\beta}(r)$ has the first and second maximum and the first and second minimum, respectively. $n_{\alpha\beta}$(m1) and $n_{\alpha\beta}$(m2) are the running integration numbers integrated up to r_{M1} and r_{M2}, respectively.

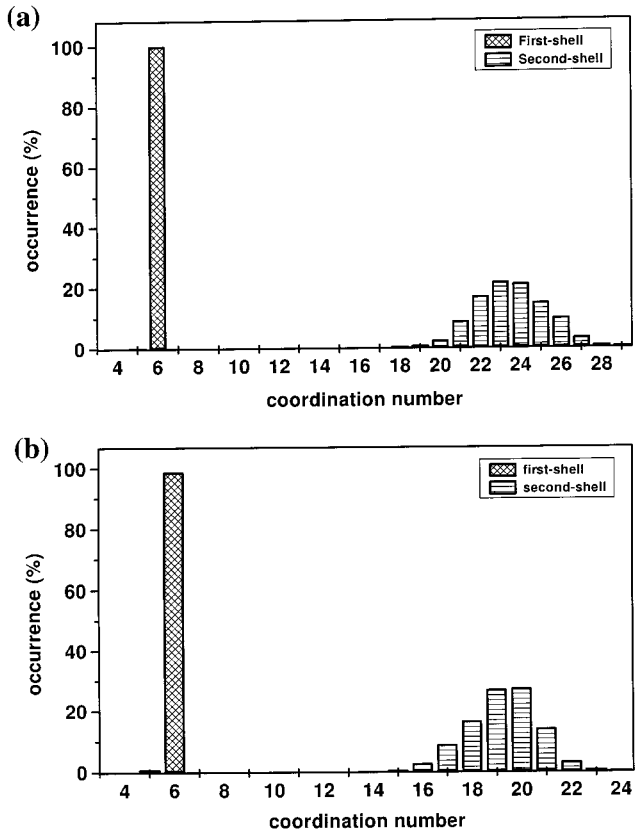

Figure 3. First- and second-shell coordination number distribution of Cu^+ in (a) liquid ammonia and (b) water.

coordination number, namely 5. The fact that the Cu−N RDF comes to zero after its first peak and stays vanishingly small for more than 1 Å suggests that the first solvation shell is stable and that ligand exchange with the second shell should be rather marginal.

The Cu−H RDF shows a sharp peak centered at 2.71 Å RDFs representing the first solvation sphere of Cu^+ in ammonia and not overlapping with the Cu−N RDF, indicating that the first solvation shell has rather a rigid structure with the nitrogens oriented toward the central ion in dipole moment direction.

The second-shell coordination number distribution of Cu^+ in liquid ammonia (Figure 3a) shows that 18 to 29 (average 23.5) ammonia molecules in this sphere interact with the 6 ammonia molecules in the first shell. This indicates that hydrogen bonding is not the exclusive factor determining the interaction of ammonia molecules between first and second solvation shell, since on average four ammonia molecules in the second shell interact with one ammonia of the first shell.

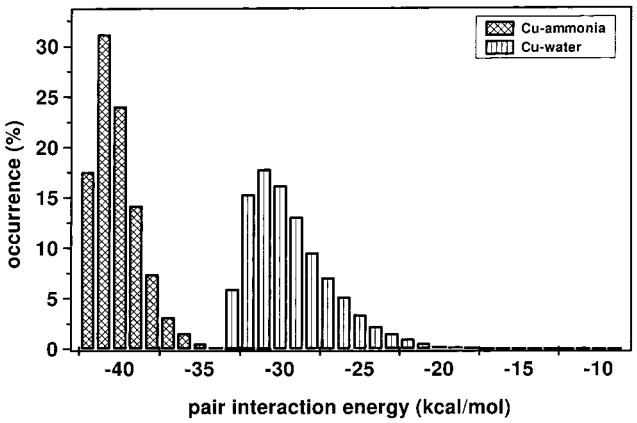

Figure 4. Distribution of Cu^+−NH_3 and Cu^+−H_2O pair interaction energies in the first shell.

For copper(I) in water, a sharp first peak is observed in the Cu−O RDF (Figure 2b), located at 2.20 Å. The coordination number distribution analysis (Figure 3b) for the first hydration shell of Cu^+ leads to 1.2% of 5 and 98.8% of 6 water molecules around Cu^+. The peak separation of the first and second hydration shell is less than 0.25 Å, and thus much smaller than in the case of Cu^+ in liquid ammonia. This indicates that ligand exchange should occur somewhat easier in water, compared to liquid ammonia.

The average coordination number of the second hydration shell, located between 3.0 and 5.41 Å, is 19.3. This reveals that ligand orientation and binding is mostly, but not exclusively determined by hydrogen bonding since on average 3.2 ligand molecules in the second shell interact with one ligand of the first shell.

The average coordination of Cu^+ both in ammonia and water was found to be an octahedral arrangement of solvent molecules in the first shell. It must be emphasized that there is an uncertainty in these results, namely the neglect of many-body interactions. In the case of Cu^{2+}, three-body corrections are essential to reproduce the correct coordination number of the first solvation shell.[15,18] Comparing, however, the interaction energies for Cu^{2+}−NH_3 (−111.7 kcal mol^{-1}) and for Cu^+−NH_3 (−43.4 kcal mol^{-1}) it can be assumed that these effects should play a much smaller role in the case of the monovalent ion.

The pair energy distributions for Cu^+−NH_3 and Cu^+−H_2O are shown in Figure 4. The average pair energy values of −40.2 kcal mol^{-1} for Cu^+−ammonia and −29.2 kcal mol^{-1} for Cu^+−water are only 4.0 kcal mol^{-1} higher than the global minima resulting from SCF calculations. These results are in a good agreement with the investigation of nonadditivity of interaction in hydrated Cu^+ clusters,[4] confirming that for Cu^+ many-body effects are much less important than for Cu^{2+}. The pair interaction energies for Cu^+−H_2O are more widely distributed than those of Cu^+−NH_3, indicating again a higher flexibility of ligand arrangements in water.

The angular distributions of NH_3−Cu−NH_3 and H_2O−Cu−H_2O up to the first minimum of Cu−N and Cu−O RDFs were evaluated and are shown in Figure 5 in order to elucidate the orientational arrangement inside the first solvation shell. The angle of the $[Cu(NH_3)_6]^+$ complex obtained from the simulation shows a sharp peak between 75° and 114° with a maximum centered at 88° and a smaller peak between 155° and 180° with

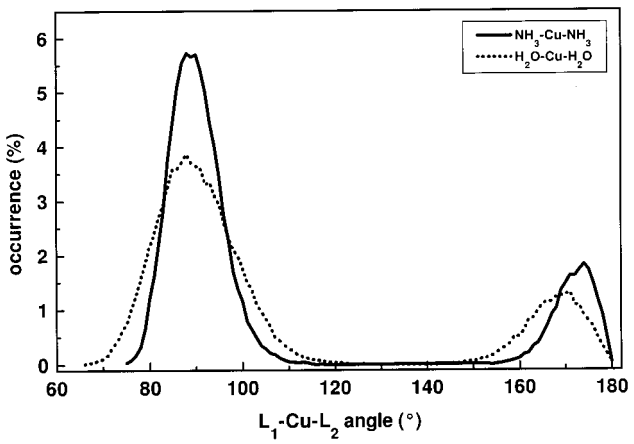

Figure 5. Distribution of bond angles $NH_3-Cu^+-NH_3$ and $H_2O-Cu^+-H_2O$.

a maximum centered at 174°. The peaks at 88° and 174° indicate that $[Cu(NH_3)_6]^+$ is a slightly distorted octahedral complex. The angles in $[Cu(H_2O)_6]^+$ are almost the same as in $[Cu(NH_3)_6]^+$, but the intensities and their widths differ to some extent. The broadness of these peaks point out again that the water molecules in the first shell are more flexible than ammonia ligands, which is easily understandable by geometrical and steric considerations, and by the lower interaction energy between Cu^+ and water, compared to the ammonia ligand.

4. Conclusion

Monte Carlo simulations using ab initio pair potential predicted six ligands in the first solvation shell of Cu^+ both in ammonia and in water, corresponding to distorted octahedral complexes.

The RDFs, coordination number distributions, and pair interaction energy distribution analyses indicated that ligand exchange reactions take place more easily in water than in liquid ammonia. In both cases, however, a nonnegligible amount of this ion has a coordination number of 5, providing easy access to a further incoming ligand.

Acknowledgment. Financial support by the Austrian Science Foundation (Project P11683-PHY) and a scholarship of the Austrian Federal Ministry for Foreign Affairs for H.D.P. are gratefully acknowledged.

References and Notes

(1) Clemmer, D. F.; Armentrout, P. B. *J. Phys. Chem.* **1991**, *95*, 3084.
(2) Magnera, T. F.; David, D. E.; Michl, J. *J. Am. Chem. Soc.* **1989**, *111*, 4100.
(3) Marinelli, P. J.; Squires, R. R. *J. Am. Chem. Soc.* **1989,** *111*, 4101.
(4) Curtiss, L. A.; Jurgens, R. *J. Chem. Phys.* **1990**, *94*, 5509.
(5) Bauschlicher, C. W., Jr.; Langhoff, S. R.; Partridge, H. *J. Chem. Phys.* **1991**, *94*, 2068.
(6) Dalleska, N. F.; Honma, K.; Sunderlin, L. S.; Armentrout, P. B. *J. Am. Chem. Soc.* **1994**, *116*, 3519.
(7) Magnusson, E.; Moriarty, N. W. *Inorg. Chem.* **1996**, *35*, 5711.
(8) Langhoff, S. R.; Bauschlicher, C. W., Jr.; Partridge, H.; Sodupe, M. *J. Phys. Chem.* **1991**, *95*, 10677.
(9) Luna, A.; Amekraz, B.; Tortajada, J. *Chem. Phys. Lett.* **1997**, *266*, 31.
(10) Hoyau, S.; Ohanessian, G. *Chem. Phys. Lett.* **1997**, *280*, 266.
(11) Holland, P. M.; Castleman, A. W., Jr. *J. Chem. Phys.* **1982**, *76*, 4195.
(12) Braish, T. F.; Duncan, R. E.; Harber, J. J.; Steffen, R. L.; Stevenson, K. L. *Inorg. Chem.* **1984**, *23*, 4072.
(13) Horvath, O.; Stevenson, K. L. *Inorg. Chem.* **1989**, *28*, 2548.
(14) Cordeiro, M. N. D. S.; Gomes, J. A. N. F. *J. Chem. Soc., Faraday Trans. 2* **1988**, *84*, 693.
(15) Texler, N. R.; Rode, B. M. *J. Phys. Chem.* **1995**, *99*, 15714.
(16) Curtiss, L. A.; Halley, J. W.; Hautman, J.; Rahman, A. *J. Chem. Phys.* **1987**, *86*, 2319.
(17) Hannongbua, S. *J. Chem. Phys.* **1997**, *106*, 6076.
(18) Pranowo, H. D.; Rode, B. M. *J. Phys. Chem. A* **1999**, *103*, 4298.
(19) Hannongbua, S. *Chem. Phys. Lett.* **1998**, *188*, 663.
(20) Probst, M. M. *Chem. Phys. Lett.* **1987**, *137*, 229.
(21) Beaggley, B.; Eriksson, A.; Lindgren, J.; Persson, I. *J. Phys.: Condens. Matter* **1989**, *1*, 2395.
(22) Schäfer, A.; Horn, H.; Ahlrichs, R. *J. Chem. Phys.* **1992**, *97*, 2571.
(23) Dunning, T. H., Jr. *J. Chem. Phys.* **1970**, *53*, 2823.
(24) Frisch, M. J.; Trucks, G. W.; Schlegel, H. B.; Gill, P. M. W.; Johnson, B. G.; Robb, M. A.; Cheeseman, J. R.; Keith, T. A.; Petersson, G. A.; Montgomery, J. A.; Raghavachari, K.; Al-Laham, M. A.; Zakrzewski, V. G.; Ortiz, J. V.; Foresman, J. B.; Cioslowski, J.; Stefanov, B. B.; Nanayakkara, A.; Challacombe, M.; Peng, C. Y.; Ayala, P. Y.; Chen, W.; Wong, M. W.; Andres, J. L.; Replogle, E. S.; Gomperts, R.; Martin, R. L.; Fox, D. J.; Binkley, J. S.; Defrees, D. J.; Baker, J.; Stewart, J. J. P.; Head-Gordon, M.; Gonzalez, C.; Pople, J. A. *Gaussian 94*; Gaussian, Inc.: Pittsburgh, PA, 1995.
(25) Benedict, W. S.; Plyler, E. K. *Can. J. Phys.* **1985**, *35*, 890.
(26) Kuchitzu, K.; Morino, Y. *Bull. Chem. Soc. Jpn.* **1965**, *38*, 814.
(27) Kerdcharoen, T.; Liedl, K. R.; Rode, B. M. *Chem. Phys.* **1996**, *211*, 313.
(28) Tongraar, A.; Hannongbua, S.; Rode, B. M. *Chem. Phys.* **1997**, *219*, 279.
(29) Hannongbua, S.; Kerdcharoen, T.; Rode, B. M. *J. Chem. Phys.* **1992**, *96*, 6945.
(30) Jancso, G.; Heinzinger, K. *Z. Naturforsch.* **1985**, *40a*, 1235.
(31) Allen, M. P.; Tiedesley, D. J. *Computer Simulation of Liquids*; Oxford University Press: Oxford, U. K., 1987.
(32) Tongraar, A.; Liedl, K. R.; Rode, B. M. *Chem. Phys. Lett.* **1998**, *286*, 56.
(33) Kerdcharoen, T. *Hot-Spot Molecular Dynamics*; Ph.D. Thesis, University of Innsbruck, Austria, 1995.
(34) Tongraar, A.; Liedl, K. R.; Rode, B. M. *J. Phys. Chem. A* **1998**, *102*, 10340.
(35) Krömer, R. T.; Michopoulos, Y.; Rode, B. M. *Z. Naturforsch*. **1991**, *45a*, 1303.
(36) Rode, B. M.; Islam, S. M. *Z. Naturforsch.* **1991**, *46a*, 357.
(37) Stevens, W. J.; Basch, H.; Krauss, M. *J. Chem. Phys.* **1984**, *81*, 6026.
(38) Wadt, W. R.; Hay, P. J. *J. Chem. Phys.* **1985**, *82*, 284.
(39) Hofmann, H. J.; Hobza, P.; Camni, R.; Tomasi, J.; Zahradnik, R. *J. Mol. Struct. (THEOCHEM)* **1989**, *201*, 339.